Journal of Life Sciences and Informatics
ISSN Online: 3106-6542 , ISSN Print: 3106-6534

Research Paper

Whole-blood RNA-seq of severe COVID-19 reveals neutrophil immunothrombosis and reduced adaptive immune and ribosomal programs

Muhammad Abrar Yousaf [1*]

[1*] Section of Biology and Genetics, Department of Neurosciences, Biomedicine and Movement Sciences, University of Verona, Verona, Italy

Correspondence: muhammadabrar.yousaf@univr.it

Abstract:

Severe coronavirus disease 2019 (COVID-19) is characterized by systemic inflammation, vascular injury, and immune dysfunction, yet the coordinated transcriptional programs underlying these processes remain incompletely resolved. Here, we re-analyzed whole-blood RNA sequencing data from 44 patients with severe COVID-19 and 10 healthy donors to identify disease-associated molecular pathways. Principal component analysis separated the two groups, and differential expression analysis identified 3,975 genes, including 2,796 upregulated and 1,179 downregulated transcripts. Upregulated genes were enriched for antimicrobial defense, innate and antiviral immunity, neutrophil extracellular trap formation, complement and coagulation, cell adhesion, extracellular matrix interactions, and cell cycle activity. Downregulated genes were dominated by ribosomal and translational programs, major histocompatibility complex class II antigen presentation, lymphocyte migration, and T-cell receptor signaling. Protein-interaction analysis further connected hub genes involved in inflammation, extracellular-matrix remodeling, cell cycling, T-cell biology, and ribosomal function. Together, these findings define severe COVID-19 as a transcriptional state of neutrophil-centered inflammation and immunothrombosis coupled to weakened adaptive immune and biosynthetic programs, providing a systems-level view of the molecular disturbances associated with severe disease.

Keywords: COVID-19, neutrophil, immunothrombosis, RNA differential expression analysis

Citation: Yousaf M A. (2026). Whole-blood RNA-seq of severe COVID-19 reveals neutrophil immunothrombosis and reduced adaptive immune and ribosomal programs. J Life Sci Inform, 2(1), 1–23.

Conflict of Interest: Author(s) declared no conflict of interest

Introduction:

Coronavirus disease 2019 (COVID-19) is an infectious disease caused by severe acute respiratory syndrome coronavirus 2 (SARS-CoV-2). Although most infected individuals experience mild or moderate respiratory illness, some patients develop severe pneumonia, hypoxemia, acute respiratory distress syndrome, and injury to organs beyond the lungs (World Health Organization [WHO], 2025). Severe COVID-19 is associated with major changes in the circulating immune system, including reduced lymphocyte and T-cell numbers, increased neutrophil counts, an elevated neutrophil-to-lymphocyte ratio, and increased concentrations of inflammatory mediators (Qin et al., 2020). The disease also affects the pulmonary vasculature. Lung tissue from patients with fatal COVID-19 has shown endothelial injury, microangiopathy, widespread microvascular thrombosis, and abnormal vascular remodeling (Ackermann et al., 2020). In addition, excessive neutrophil extracellular trap formation may promote interactions among neutrophils, platelets and coagulation factors, thereby contributing to pulmonary immunothrombosis and respiratory failure (Middleton et al., 2020). These observations indicate that severe COVID-19 is not limited to viral injury of the respiratory epithelium but involves interconnected immune, inflammatory, vascular, and coagulation abnormalities.

The simultaneous involvement of multiple biological systems makes it difficult to explain severe COVID-19 with individual laboratory markers or a limited set of candidate genes. RNA sequencing provides an unbiased method for measuring gene expression across the transcriptome and enables differentially expressed genes to be connected with broader biological functions and molecular pathways (Conesa et al., 2016). Whole blood is particularly relevant for examining severe COVID-19 because it contains circulating immune cells and molecular signals related to systemic inflammation, antimicrobial defense, coagulation, and vascular responses. However, the relationships among these processes, particularly innate and adaptive immunity, cell adhesion, platelet and vascular activity, and extracellular-matrix-associated pathways, remain insufficiently integrated within a single biological framework. Therefore, the present study was conducted to characterize the whole-blood transcriptional response associated with severe COVID-19 and to identify the genes, biological processes, and signaling pathways that distinguish patients with severe disease from healthy individuals. This approach may provide a clearer molecular explanation of how systemic immune dysregulation and vascular pathology develop together during severe COVID-19.

Material and Methods

Data

The whole-blood RNA-seq dataset GSE171110 was obtained from NCBI GEO (Edgar et al., 2002). The dataset was chosen using five criteria: (i) samples from Homo sapiens, (ii) no in vitro drug treatment, (iii) no cell lines, (iv) comparison of normal versus disease conditions, and (v) more than four samples in total. The dataset was generated on the Illumina HiSeq 2500 platform (GPL16791) and contained 54 samples: 44 from patients with severe COVID-19 and 10 from

healthy donors. RNA-seq counts and sample annotations were downloaded from GEO and grouped by clinical status to identify transcriptional changes associated with severe COVID-19.

RNA-seq analysis workflow

Galaxy was used to perform RNA-seq analysis (Goecks et al., 2010) (Figure 1). Raw FASTQ files were evaluated using FastQC for sequence quality metrics, including GC content, read length distribution, and adapter contamination (Andrews, 2010). Reads of higher quality were aligned to the GRCh38/hg38 reference genome using the splice-aware HISAT aligner (Kim et al., 2015). Post-alignment quality was assessed using RSeQC (Wang et al., 2012), and PCR duplicates were identified with MarkDuplicates and removed with SAMtools RmDup (Li et al., 2009). featureCounts then generated the gene-level counts (Liao et al., 2014).

Finally, differential expression was assessed using DESeq2 (Love et al., 2014), in which count data were modeled with a negative binomial distribution and shrinkage estimates were applied to dispersion and fold change (Anders & Huber, 2010). Genes were classified as significantly differentially expressed when they showed a log2 fold change greater than 1 or less than -1, and an adjusted p-value below 0.05.

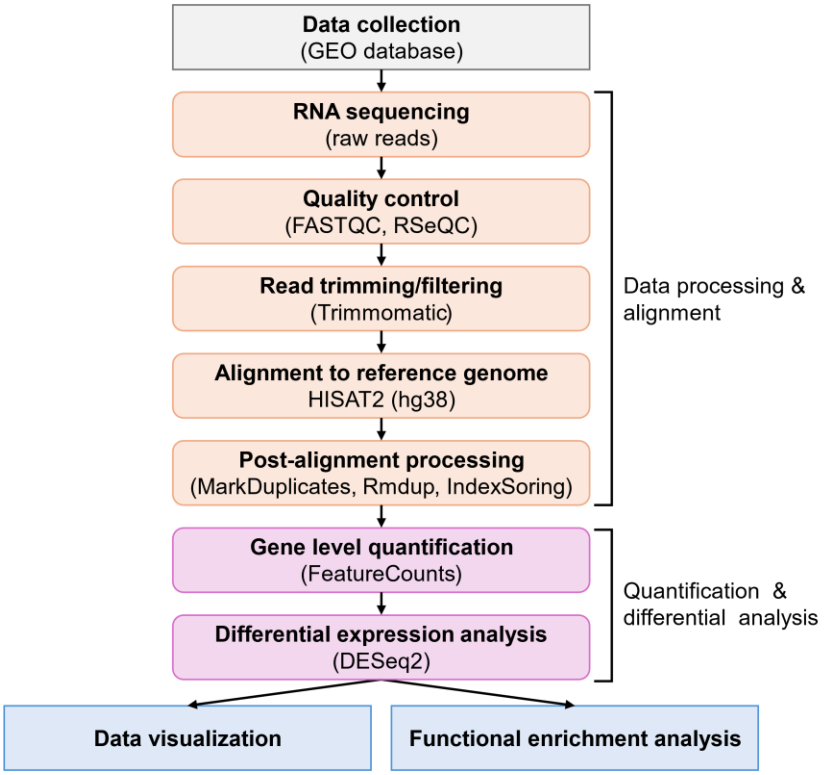

Figure 1. Overview of the RNA-seq analysis pipeline. A schematic representation of the computational workflow used in this study. RNA-seq data were collected from the GEO database and subjected to quality control (FASTQC, RSeQC), followed by alignment to the human reference genome (hg38) using HISAT2. Post-alignment processing was performed with MarkDuplicates and Rmdup to remove duplicate reads. Gene expression counts were obtained with FeatureCounts, and differential expression analysis was carried out using DESeq2. Results were visualized and examined through functional enrichment analysis.

Functional-enrichment analysis

Gene Ontology biological process and Kyoto Encyclopedia of Genes and Genomes pathway enrichment analyses were performed using the DAVID Functional Annotation Tool (Dennis et al., 2003; Sherman et al., 2022). Upregulated and downregulated protein-coding genes were analyzed separately, with Homo sapiens selected as the background species. Enrichment significance was calculated using DAVID modified Fisher's exact test, also known as the EASE score, and corrected for multiple testing using the Benjamini-Hochberg method. Terms and pathways with an adjusted p-value or FDR below 0.05 were considered significantly enriched. Significant results were summarized by fold enrichment, adjusted p-value/FDR, and number of contributing genes.

Protein-protein interaction network and hub-gene identification

Significantly differentially expressed protein-coding genes were used to construct a protein–protein association network using the STRING database, with Homo sapiens selected as the organism. Only associations with a combined confidence score of at least 0.700 were retained, corresponding to a high-confidence interaction threshold (Szklarczyk et al., 2023). The resulting network was exported from STRING and imported into Cytoscape for visualization and topological analysis (Shannon et al., 2003). Candidate hub genes were identified using the cytoHubba application in Cytoscape. Nodes were ranked using the Degree algorithm, which measures the number of direct connections between each protein and the other proteins in the network. The ten proteins with the highest degree scores were selected as candidate hub genes (Chin et al., 2014). Hub-gene selection was based only on network connectivity and was independent of the direction or magnitude of differential expression.

Results and discussion

Principal component analysis of the transformed expression data separated samples from patients with severe COVID-19 from those of healthy donors. PC1 and PC2 explained 26.48% and 10.13% of the total variance, respectively (Figure 2A). Healthy donor samples clustered closely, whereas samples from patients with severe COVID-19 were more widely distributed, consistent with greater heterogeneity in their whole-blood expression profiles.

The distributions of transformed expression values were similar across all 54 samples, with comparable medians and interquartile ranges (Figure 2B). No sample showed a marked shift in its overall expression distribution after transformation. Together, these findings indicate that disease status was a major source of variation in the whole-blood transcriptome and that expression profiles were more heterogeneous among patients with severe COVID-19.

As an additional sample-level consistency check, we examined the normalized expression of GAPDH (Figure 3A) and ACTB (Figure 3B) across all samples. No statistically significant differences were detected between patients with severe COVID-19 and healthy donors based on log2 fold change. This result indicates that neither gene showed evidence of differential expression in this dataset.

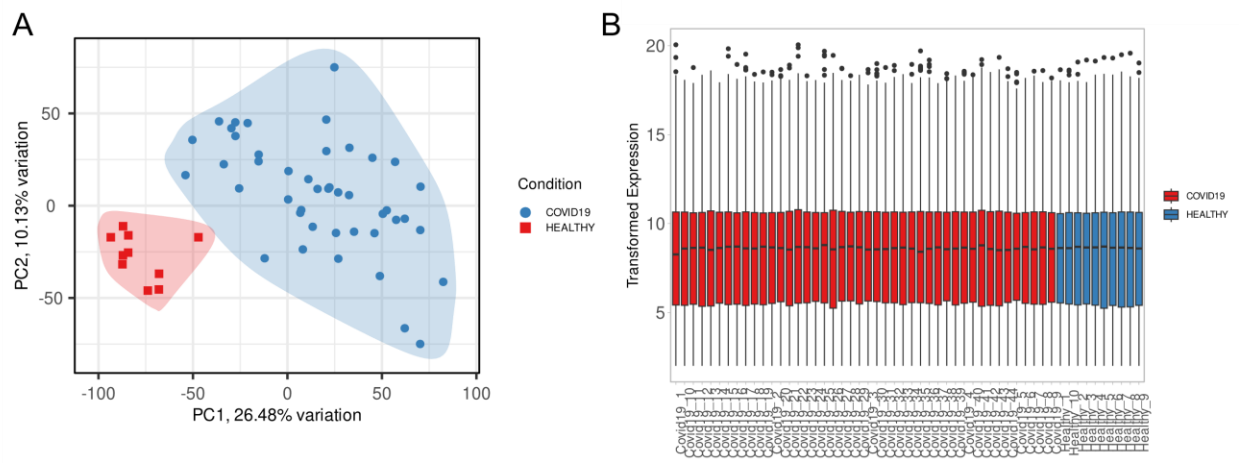

Figure 2. Global expression patterns and sample-level distributions in severe COVID-19 and healthy donors. (A) Principal-component analysis of transformed whole-blood RNA-seq expression data from patients with severe COVID-19 and healthy donors. Each symbol represents one sample. PC1 and PC2 explained 26.48% and 10.13% of the total variance, respectively. Shaded ellipses summarize the distribution of samples within each group. (B) Sample-wise distributions of transformed expression values across all 54 samples. Boxes indicate the interquartile range, horizontal lines indicate the median, whiskers extend to 1.5 times the interquartile range, and individual points represent values beyond the whiskers.

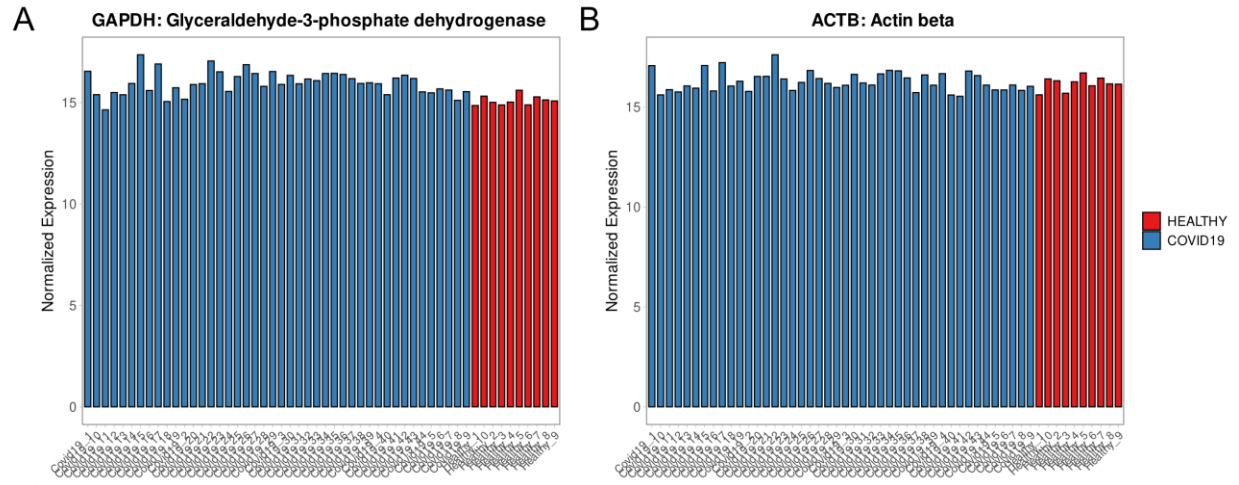

Figure 3. Normalized expression of GAPDH and ACTB across severe COVID-19 and healthy donor samples. Bar plots show normalized whole-blood RNA-seq expression values for (A) GAPDH (left) and (B) ACTB (right) in individual samples. Samples from patients with severe COVID-19 are shown in blue, and samples from healthy donors are shown in red. Both genes displayed broadly comparable expression ranges across the two groups, with no marked group-level shift.

Severe COVID-19 is associated with broad changes in the whole-blood transcriptome

To define the transcriptional changes associated with severe COVID-19, we compared whole-blood RNA-seq profiles from 44 patients with severe disease and 10 healthy donors. The analysis

included 18,726 annotated genes and RNA features. Most were protein-coding genes (14,429), followed by non-coding RNA genes (3,195), pseudogenes (664), and smaller RNA classes (**Figure 4A**).

Differential-expression analysis identified 3,975 genes that differed significantly between severe COVID-19 and healthy donors. Of these, 2,796 were upregulated and 1,179 were downregulated in severe disease (**Figure 4B**). The larger number of upregulated genes indicates that severe COVID-19 was associated predominantly with increased transcription of specific gene programs, although substantial reductions in gene expression were also present. Hierarchical clustering of the top 1,000 differentially expressed genes revealed coordinated expression differences across the study samples (**Figure 4C**). Healthy donor samples showed relatively similar expression profiles, whereas severe COVID-19 samples displayed broader variation. Despite this patient-to-patient heterogeneity, the overall expression pattern distinguished most severe COVID-19 samples from healthy donors.

The volcano plot showed both the magnitude and statistical significance of these expression differences (**Figure 4D**). Upregulated genes were distributed across a broad range of positive $\log_2$ fold change, whereas a smaller group of genes showed significant negative $\log_2$ fold change, showing downregulation. Several strongly upregulated genes, including MKI67, MYBL2, and SDC1, were among the most prominent signals. In contrast, several ribosomal genes, including RPS14, RPL30, and RPS27A, were among the downregulated genes. These individual genes provide examples of the wider transcriptional patterns but should be interpreted within the context of pathway-level analyses.

Together, these findings demonstrate extensive remodeling of the whole-blood transcriptome in severe COVID-19. The predominance of upregulated genes suggests strong activation of disease-associated transcriptional programs, while the downregulated genes indicate suppression or reduced representation of other biological processes. Because the analysis was performed in bulk whole blood, these differences may reflect both changes in gene regulation within individual cells and changes in the proportions of circulating blood-cell populations. The differentially expressed genes were therefore examined further using Gene Ontology and pathway-enrichment analyses to identify the biological processes underlying these global expression changes.

Upregulated genes reveal coordinated antimicrobial, innate immune, antiviral, adhesion, and cell-cycle programs in severe COVID-19

Gene Ontology biological process enrichment analysis was performed on upregulated protein-coding genes. The top enriched terms described a coordinated response involving antimicrobial defense, innate immune activation, inflammation, antiviral activity, cell adhesion, and cell division (Figure 5A).

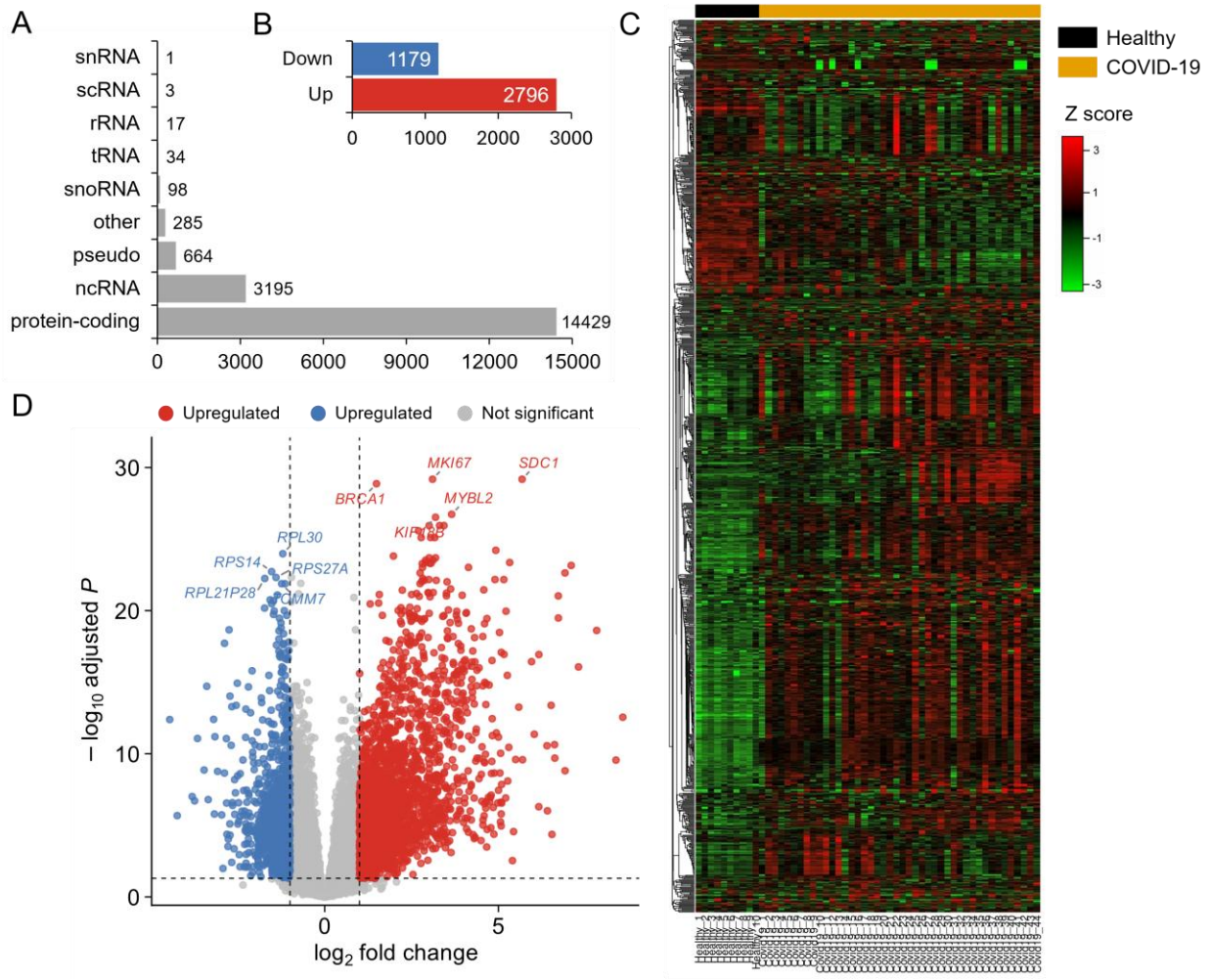

Figure 4. Differential gene-expression landscape of severe COVID-19 in whole blood. (A) Distribution of the 18,726 annotated features included in the analysis. Most features were protein-coding genes (14,429), followed by non-coding RNAs (3,195), pseudogenes (664), and smaller RNA classes. (B) Numbers of differentially expressed genes in severe COVID-19 relative to healthy donors, comprising 2,796 upregulated and 1,179 downregulated genes. (C) Heatmap of the top 1,000 differentially expressed genes across 44 severe COVID-19 samples and 10 healthy donor samples. Rows represent genes and columns represent individual samples. Colors show row-scaled relative expression, from lower expression in green to higher expression in red; genes were grouped by hierarchical clustering, and the upper annotation denotes the clinical group. (D) Volcano plot showing the magnitude and statistical significance of gene-expression differences. Red points indicate upregulated genes, blue points indicate downregulated genes, and grey points indicate genes that did not meet the differential-expression thresholds. Dashed lines mark the applied fold-change and adjusted-significance cut-offs; selected genes are labeled.

Innate immune response in mucosa

Innate immune response in mucosa was the most strongly enriched biological process. It contained 21 genes, showed a 7.47-fold enrichment, and had an FDR of 5.70 × 10−10. The gene set included the antimicrobial peptides DEFA1, DEFA1B, DEFA3, and CAMP, together with

RNASE2, RNASE3, and LTF. These proteins contribute to the rapid defense against invading microorganisms through direct antimicrobial activity, membrane disruption, and sequestration of nutrients required for microbial growth.
The term also contained 13 H2B histone-cluster genes, including H2BC4, H2BC5, H2BC6, H2BC7, H2BC8, H2BC9, H2BC11, H2BC12, H2BC12L, H2BC15, H2BC17, H2BC18 and H2BC21. In this whole-blood dataset, the combination of histone genes, defensins, ribonucleases, and lactoferrin defines a strong extracellular and granulocyte-associated antimicrobial signature.
This pattern is consistent with blood transcriptome studies that identified increased expression of defensins, lactoferrin, ribonucleases, and other granulocyte-associated genes in severe COVID-19. These signatures were particularly prominent in patients with severe disease and were reproduced in purified granulocyte samples, supporting a major contribution from the circulating granulocyte compartment (Aschenbrenner et al., 2021; Prebensen et al., 2023).

Antibacterial humoral response

Antibacterial humoral response included 28 genes, showed a 4.36-fold enrichment, and had an FDR of 1.29 × 10−7. This term was enriched by soluble antimicrobial molecules and granulocyte granule proteins, including DEFA1, DEFA1B, DEFA3, DEFA4, CAMP, BPI, AZU1, CTSG, LTF, RNASE3, SLPI, and ANG. Many of the H2B histone genes identified in the mucosal innate immune term were also present. The gene composition indicates increased expression of soluble components of innate antimicrobial defense. Defensins and cathelicidin can directly damage microbial membranes, whereas BPI binds bacterial lipopolysaccharide and has antimicrobial activity. Lactoferrin limits microbial growth by binding iron, and azurocidin, cathepsin G, and RNASE3 are stored in granulocyte granules and contribute to antimicrobial defense.
The enrichment of these genes is consistent with the strong granulocyte response described in severe COVID-19. Aschenbrenner et al. (2021) reported increased expression of several of the same antimicrobial and granule-associated genes in severe disease. Prebensen et al. (2023) similarly identified a severity-associated module containing LTF, BPI, AZU1, DEFA3, and DEFA4 that increased over the course of severe disease.

Cell adhesion

Cell adhesion was the largest enriched term by gene count. It contained 94 genes, showed a 1.91-fold enrichment, and had an FDR of 2.40 × 10−6. The term included genes involved in leukocyte adhesion, platelet interactions, vascular structure, and extracellular-matrix attachment. Leukocyte-associated genes included ITGAM, ITGAX, SELL, FERMT3, CEACAM1, SIRPA, CD177, SIGLEC1, SIGLEC5, SIGLEC9, and SIGLEC16. These genes regulate immune-cell attachment, migration, recognition, and signaling. Their increased expression indicates substantial remodeling of the adhesive and migratory properties of circulating immune cells. The term also contained the platelet-associated genes ITGA2B, ITGB3, GP1BA, GP1BB, GP9, SELP, and THBS1. These genes encode major platelet receptors and adhesion molecules involved in platelet attachment, aggregation, and communication with leukocytes and the vascular wall. Vascular-associated genes included VWF, CDH5, CLDN5, EGFL7, JCAD and MMRN1, while extracellular-matrix genes included FN1, TNC, COL1A1, COL6A3, COL7A1, LAMB1, LAMB3 and LAMC1. Together, this mixed gene set indicates increased communication among leukocytes, platelets, vascular-associated cells, and the extracellular matrix. Similar transcriptional modules involving platelet activation, aggregation, coagulation, cell-cell adhesion, and integrin signaling have been reported in severe COVID-19 (Aschenbrenner et al., 2021). Longitudinal analysis also identified a platelet-associated module containing ITGB3,

GP1BB, TBXA2R, and GP6 that was consistently more highly expressed in severe disease (Prebensen et al., 2023). These findings connect the adhesion-related expression pattern with the thrombo-inflammatory response that characterizes severe COVID-19.

Negative regulation of viral genome replication

Negative regulation of viral genome replication contained 19 genes, showed a 5.14-fold enrichment, and had an FDR of 7.17 × 10−6. The term included the viral RNA sensor IFIH1, which encodes MDA5, as well as several interferon-stimulated antiviral genes. IFITM1, IFITM2, and IFITM3 encode membrane-associated proteins that restrict viral entry and membrane fusion. MX1 and RSAD2 interfere with viral replication, while ISG15 modifies cellular and viral proteins during the antiviral response. OAS1, OAS2, OAS3, and OASL participate in the recognition and degradation of viral RNA. The term also contained EIF2AK2, IFIT1, PLSCR1, TRIM6, and APOBEC3A, which contribute to antiviral sensing, translation control, and restriction of viral replication. The coordinated increase in these genes indicates a strong interferon-linked antiviral transcriptional program in severe COVID-19. Single-cell analysis has identified heterogeneous yet prominent interferon-stimulated gene expression across immune cell populations in patients with severe disease (Wilk et al., 2020). Longitudinal whole-blood analysis also detected strong enrichment of IFIT, ISG15, OAS, and APOBEC genes, particularly during the early stages of infection (Prebensen et al., 2023). In addition, longitudinal immune profiling showed that type 1 antiviral responses remained elevated in many patients with severe disease (Lucas et al., 2020).

Innate immune response

Innate immune response contained 86 genes, showed a 1.88-fold enrichment, and had an FDR of 1.53 × 10−5. This broad term encompasses genes involved in pathogen recognition, complement activity, Fc receptor signaling, antimicrobial defense, and myeloid inflammation. Pattern-recognition genes included TLR2, TLR4, TLR5, CLEC4E, CLEC5A, NLRC4, NAIP, AIM2 and IFIH1. These receptors detect microbial or danger-associated molecules and initiate intracellular inflammatory and antiviral responses. Complement- and Fc-receptor-associated genes included C1QA, C1QB, C1QC, C1RL, C2, CR1, FCGR1A, and FCER1G, indicating increased activity of antibody-dependent and complement-associated innate immune programs. The term also contained the inflammatory alarmins S100A8, S100A9 and S100A12, together with PGLYRP1, CAMP, BPI, LCN2, PTX3, MARCO, PADI4, CD177 and ARG1. These genes are strongly associated with activated, inflammatory, and immature neutrophil states.

This result closely matches previous transcriptomic studies of severe COVID-19. Aschenbrenner et al. (2021) identified CD177, ELANE, MPO, OLFM4, S100A8, S100A9, and S100A12 among the most prominent severity-associated genes. Single-cell profiling also identified developing neutrophil populations in patients with acute respiratory failure (Wilk et al., 2020). Prebensen et al. (2023) further described two neutrophil-associated transcriptional trajectories, including a later program enriched in ELANE, BPI, AZU1, LTF, LCN2, DEFA3, and DEFA4. Together, these studies support extensive activation and restructuring of the circulating innate immune compartment in severe disease.

Chromosome segregation

Chromosome segregation contained 29 genes, showed a 3.28-fold enrichment, and had an FDR of 2.45 × 10−5. Representative genes included TOP2A, MKI67, TTK, BUB1, NDC80, NUF2, CENPE, CENPF, BIRC5, SKA1, SKA3, SPC24 and SPC25. These genes regulate chromosome organization and movement during cell division. MKI67 is widely expressed in proliferating cells,

while TOP2A regulates DNA topology during replication and mitosis. TTK and BUB1 contribute to the mitotic checkpoint, and NDC80, NUF2, SKA1, SKA3, SPC24, and SPC25 form or support the kinetochore machinery that connects chromosomes to the mitotic spindle. CENPE, CENPF, and BIRC5 also support chromosome alignment, separation, and cell survival during mitosis. The coordinated expression of these genes indicates an increased proliferative signal in the blood of patients with severe COVID-19. Blood transcriptome studies have similarly reported increased expression of cell-cycle progression genes in COVID-19, including those involved in DNA replication and mitotic control (Aschenbrenner et al., 2021). This signal is consistent with the expansion of cycling immune or precursor-cell populations during the systemic response to severe infection.

Defense response to bacterium

The defense response to the bacterium contained 38 genes, showed a 2.69-fold enrichment, and had an FDR of $3.32 \times 10{-}5$. The gene set included neutrophil granule proteins and antimicrobial effectors such as MPO, ELANE, PGLYRP1, CAMP, AZU1, LCN2 and DEFA3. It also contained microbial-recognition and inflammatory genes, including TLR4, NLRC4, NAIP, CLEC4D, CLEC4E, FPR2, FCGR1A, S100A8, S100A9, and S100A12. These genes support microbial sensing, phagocyte recruitment, granule release, and inflammatory signaling. The strong contribution of MPO, ELANE, AZU1, LCN2, defensins, and S100-family genes links this term to the neutrophil-dominated response in severe COVID-19. Aschenbrenner et al. (2021) identified the same granulocyte and alarmin genes among the most strongly increased transcripts in severe cases. Prebensen et al. (2023) also found that modules containing ELANE, BPI, AZU1, LTF, LCN2, DEFA3, and DEFA4 were associated with disease severity and an increasingly immature circulating neutrophil phenotype.

Inflammatory response

Inflammatory response included 73 genes, showed a 1.95-fold enrichment, and had an FDR of $3.32 \times 10{-}5$. The term contained genes involved in inflammatory sensing, cytokine responses, complement signaling and immune-cell recruitment. Pattern-recognition genes included TLR2, TLR4, TLR5 and NLRC4. Complement and chemoattractant receptors included C3AR1, C5AR1, FPR1, and FPR2. Cytokine- and chemokine-related genes included IL1R1, IL1RN, IL18R1, IL18RAP, CXCL3, CCL3L3 and CCL25. The presence of IL1R1 and IL18R1 indicates increased responsiveness to inflammatory cytokines, while CXCL3 and CCL3L3 contribute to the recruitment and activation of myeloid cells. The term also included S100A8, S100A9, S100A12, AZU1, PTX3, VNN1, OLR1 and ACOD1. These genes are characteristic of inflammatory responses by monocytes and neutrophils. S100A8, S100A9, and S100A12 act as damage-associated inflammatory signals, whereas PTX3 contributes to innate recognition and complement regulation. This expression profile is consistent with studies showing that severe COVID-19 is accompanied by sustained systemic inflammation and the expansion of inflammatory myeloid populations. Aschenbrenner et al. (2021) identified inflammatory and neutrophil-enriched transcriptional modules in severe cases, while Lucas et al. (2020) showed that patients with severe disease maintained elevated inflammatory and antiviral immune responses over time. The enrichment, therefore, reflects a broad systemic inflammatory response involving microbial sensing, complement activity, cytokine signaling, and myeloid-cell recruitment.

Mitotic sister chromatid segregation

Mitotic sister chromatid segregation contained 16 genes, showed a 5.38-fold enrichment, and had an FDR of 3.42 × 10−5. The gene set included PLK1, CDCA8, KNL1, TUBG1, SKA1, SKA3, NDC80, ZWINT, KIF18A, KIF18B, ESPL1, KIFC1, CENPI, NUSAP1 and KIF2C. These genes form a tightly connected mitotic program. PLK1 regulates entry into and progression through mitosis. KNL1, NDC80, SKA1, SKA3, and ZWINT support kinetochore assembly and chromosome attachment to the spindle. KIF18A, KIF18B, KIFC1, and KIF2C regulate microtubule movement and chromosome positioning, while ESPL1 enables the final separation of sister chromatids. The enrichment of this term strengthens the evidence for increased cell division in severe COVID-19. Together with the chromosome-segregation term, it identifies a coherent transcriptional program involving mitotic checkpoint control, spindle organization, and chromosome separation. This is consistent with the increased expression of cell-cycle-associated genes reported in independent blood transcriptome studies of COVID-19 (Aschenbrenner et al., 2021).

Defense response to Gram-positive bacterium

The defense response to Gram-positive bacterium contained 33 genes, showed a 2.85-fold enrichment, and had an FDR of 4.71 × 10−5. The term included the antimicrobial genes DEFA1, DEFA1B, DEFA3, DEFA4, CAMP, PGLYRP1, CTSG, RNASE3 and LTF. TLR2, which recognizes several microbial cell-wall components, was also included, together with the inflammatory genes C5AR1, IL18R1, IL18RAP, FGR, and ADAM17. The term additionally contained several H2B histone-cluster genes that also contributed to the mucosal innate and antibacterial humoral response categories. The combined expression of defensins, cathelicidin, granule proteases, lactoferrin, ribonucleases, and microbial-recognition receptors indicates a strong granulocyte-associated antimicrobial program. The same antimicrobial genes have been repeatedly identified in neutrophil signatures associated with severe COVID-19. In particular, DEFA3, DEFA4, LTF, BPI, and AZU1 were part of a neutrophil-associated module that correlated with clinical severity and increased over time in severe disease (Prebensen et al., 2023).

Together, the ten enriched GO terms show that the upregulated transcriptome in severe COVID-19 was dominated by antimicrobial, neutrophil-associated, and broader myeloid-inflammatory programs. Defensins, granule proteins, histones, S100-family genes, and pattern-recognition receptors contributed repeatedly to the innate immune, antibacterial, and inflammatory categories. This response was accompanied by increased expression of interferon-stimulated antiviral genes, including IFITM1-3, MX1, RSAD2, ISG15, and OAS1-3. The cell-adhesion term added distinct platelet, vascular, and extracellular matrix components, while the chromosome-segregation terms identified a coordinated proliferative program. Overall, the results define a severe-COVID-19-associated whole-blood transcriptional state characterized by strong granulocyte and innate immune activation, sustained inflammatory and antiviral responses, increased platelet–vascular interaction programs, and expansion of cell-cycle-associated expression. This integrated pattern is consistent with the extensive restructuring of circulating immune-cell states reported in independent whole-blood and single-cell studies of severe disease (Aschenbrenner et al., 2021; Lucas et al., 2020; Prebensen et al., 2023; Wilk et al., 2020).

Downregulated genes reveal reduced translation, antigen presentation, immune-cell migration, and T-cell programs in severe COVID-19

Gene Ontology biological process analysis of downregulated genes (Figure 5A) identified the top-enriched terms, which formed three main biological patterns: reduced expression of ribosomal and translation-related genes; lower antigen presentation and broader immune-response signals;

and reduced expression of genes involved in T-cell activation, receptor signaling, and immune-cell migration.

Cytoplasmic translation

Cytoplasmic translation was the most strongly enriched downregulated process. It contained 53 genes, showed a 15.16-fold enrichment, and had an FDR of 6.42 × 10−46. Almost all genes in this term encoded components of the cytoplasmic ribosome, including large-subunit genes such as RPL3, RPL4, RPL5, RPL6, RPL10, RPL11, RPL13, RPL15, RPL17, RPL19, RPL23A, RPL24, RPL26 and RPL30, together with small-subunit genes such as RPS3, RPS5, RPS6, RPS7, RPS8, RPS10, RPS12, RPS14, RPS16, RPS17, RPS18, RPS20 and RPS23. The gene set also included UBA52 and RPS27A, which encode ubiquitin fused to ribosomal proteins. Their coordinated downregulation indicates a marked reduction in transcripts encoding the structural machinery of cytoplasmic protein synthesis.

A similar reduction in translation- and ribosome-related gene sets has been observed in longitudinal whole-blood studies of COVID-19. Prebensen et al. (2023) found that translation, RNA processing, and ribosome biogenesis programs were consistently underrepresented in patients with COVID-19, and that a ribosome biogenesis module was inversely associated with disease severity. The strong enrichment observed here indicates that reduced ribosomal gene expression is a major component of the severe-COVID-19 whole-blood transcriptome.

Translation

The broader translation term contained 57 genes, showed a 6.55-fold enrichment, and had an FDR of 1.50 × 10−26. It included nearly all ribosomal genes present in the cytoplasmic-translation category, together with additional genes involved in translational elongation and transfer RNA function. EEF1A1 encodes a central component of the translation-elongation machinery, while PSTK participates in the formation of selenocysteine-charged transfer RNA. The term also included the sex-linked ribosomal genes RPS4X, RPS4Y1, and RPS4Y2, as well as UBA52 and numerous large- and small-subunit ribosomal genes. The close overlap between the translation and cytoplasmic-translation terms shows that both were driven by the same broad reduction in ribosomal transcripts. This pattern indicates lower representation of the molecular machinery required for protein synthesis in severe COVID-19. Previous whole-blood analysis similarly reported persistent under-representation of translation-related programs throughout hospitalization, supporting the presence of a sustained change in protein-synthesis-associated gene expression (Prebensen et al., 2023).

Negative regulation of myoblast fusion

Negative regulation of myoblast fusion contained 27 genes, showed a 15.45-fold enrichment, and had an FDR of 2.90 × 10−22. Despite the name of the term, 26 of its 27 genes were ribosomal protein genes or ribosome-associated genes. These included RPL3, RPL4, RPL5, RPL6, RPL9, RPL10, RPL10A, RPL11, RPL12, RPL13, RPL13A, RPL15, RPL17, RPL18A, RPL19, RPL21, RPL23A, RPL24, RPL27A, RPL30, RPL31, RPL32, RPL34, RPL35A, RPL39 and UBA52. These ribosomal genes are implicated in the negative regulation of myoblast fusion because they drive ribosome biogenesis and the generalized protein synthesis required to maintain myoblasts in an active state of cell proliferation (Figueiredo & McCarthy, 2019). Consequently, these standard ribosomal proteins must be downregulated or structurally remodeled to allow myoblasts to exit the cell cycle and initiate the fusion process into multinucleated myotubes (Lyu & Jiang, 2022).

Striated muscle contraction

Striated muscle contraction contained 28 genes, showed an 11.31-fold enrichment, and had an FDR of 9.65 × 10−19. Twenty-seven of the genes were the same ribosomal or ribosome-associated genes found in the negative-regulation-of-myoblast-fusion term. The only clearly muscle-related gene was RYR1, which encodes a calcium-release channel required for excitation-contraction coupling in skeletal muscle. The term was therefore dominated by downregulated ribosomal genes, including RPL3, RPL4, RPL5, RPL6, RPL9, RPL10, RPL11, RPL12, RPL13, RPL15, RPL17, RPL18A, RPL19, RPL21, RPL23A, RPL24, RPL27A, RPL30, RPL31, RPL32, RPL34, RPL35A, RPL39, RPLP2, and UBA52. These ribosomal genes are also associated with striated muscle contraction, as they expand cellular translation capacity to meet the intensive protein-synthesis demands of active sarcomeres (Figueiredo & McCarthy, 2019). Furthermore, specialized variations within these ribosomal complexes, such as the dynamic interplay between RPL3 and its muscle-specific paralog, RPL3L, directly control translation elongation, thereby regulating muscle mass and maintaining cardiac contractility (Shiraishi et al., 2023).
The systemic inflammation triggered by respiratory SARS-CoV-2 infection strongly downregulates ribosomal protein and mitochondrial genes, leading to a severe translational blockade that impairs the synthesis of crucial sarcomeric components (Homma et al., 2024). This suppression of the protein-manufacturing machinery leads to myofibrillar disarray, Z-disc loss, and decreased neuromuscular efficiency, which clinically manifests as acute muscle wasting and persistent fatigue (Meacci et al., 2022).

Immune response

Immune response contained 57 genes, showed a 2.71-fold enrichment, and had an FDR of 1.43 × 10−8. The gene set included several components of adaptive immunity, particularly genes associated with antigen presentation, T-cell identity, lymphocyte migration, and immune-cell communication. MHC class II genes included HLA-DPA1, HLA-DPB1, HLA-DQA1, HLA-DQA2, HLA-DQB2, HLA-DRA, HLA-DRB1, HLA-DMB and HLA-DOA. These genes encode proteins required for the processing and presentation of extracellular antigens to CD4 T cells. T-cell-associated genes included CD2, CD4, CD8A, CD8B, CD8B2, CD28, CD40LG, TCF7, IL7R, CTSW, GZMA, STAT4 and ETS1. Several of these genes are central to T-cell development, survival, co-stimulation, and effector function. Chemokine receptors and migration-related genes included CCR3, CCR4, CCR6, CCR7, CCR9, CXCR5, CXCR6 and GPR183, while XCL1, XCL2, CCL20 and CCL28 encode immune-cell-recruiting chemokines. The coordinated reduction of these genes indicates a weaker adaptive immune transcriptional signal in severe COVID-19. Longitudinal whole-blood analysis has similarly shown reduced class II HLA expression, lower T-cell receptor signaling, and reduced estimated CD4 and CD8 T-cell proportions in COVID-19, with the strongest changes generally occurring in severe disease (Prebensen et al., 2023). Single-cell studies have also identified lymphopenia, HLA class II downregulation, and extensive reconfiguration of the circulating immune-cell compartment in severe COVID-19 (Wilk et al., 2020).

Ribosomal small-subunit biogenesis

Ribosomal small-subunit biogenesis contained 17 genes, showed a 5.99-fold enrichment, and had an FDR of 8.06 × 10−6. The term was composed almost entirely of genes encoding proteins of the 40S ribosomal subunit, including RPS3A, RPS4X, RPS5, RPS6, RPS7, RPS8, RPS12, RPS13, RPS14,

RPS15A, RPS16, RPS17, RPS23, RPS25, RPS27, and RPS27A. AK5 was the only non-ribosomal gene in the category. These proteins contribute to the assembly and function of the small ribosomal subunit, which decodes messenger RNA during translation. Their coordinated downregulation indicates reduced expression of genes required for 40S subunit formation. This result complements the strong enrichment of cytoplasmic translation and translation terms and shows that the downregulated ribosomal program involved both mature ribosome components and genes annotated to ribosome assembly. Prebensen et al. (2023) also identified persistent suppression of ribosome-biogenesis programs and an inverse association between ribosomal-module expression and COVID-19 severity.

Peptide antigen assembly with MHC class II protein complex

Peptide antigen assembly with MHC class II protein complex contained nine genes, showed a 15.45-fold enrichment, and had an FDR of $1.22 \times 10{-}5$. The gene set consisted entirely of MHC class II genes: HLA-DPA1, HLA-DPB1, HLA-DQA1, HLA-DQA2, HLA-DQB2, HLA-DRA, HLA-DRB1, HLA-DMB, and HLA-DOA. HLA-DP, HLA-DQ, and HLA-DR molecules bind peptides derived from extracellular proteins and display them to CD4 T cells. HLA-DMB supports peptide loading onto MHC class II molecules, while HLA-DOA regulates the peptide-exchange process. Their coordinated downregulation indicates lower expression of the molecular machinery required for class II antigen presentation. This pattern closely agrees with previous studies of severe COVID-19. Saichi et al. (2021) identified reduced MHC class II-related gene expression and lower activity of the MHC class II transcriptional regulator in circulating CD1c-positive dendritic cells. Wilk et al. (2020) also reported HLA class II downregulation in peripheral immune cells. Longitudinal whole-blood analysis found that class II HLA antigen-presentation programs were consistently reduced and were most strongly downregulated in severe disease (Prebensen et al., 2023).

Together, these findings indicate a prominent reduction in the antigen-presentation program of circulating blood cells during severe COVID-19.

Cell chemotaxis

Cell chemotaxis contained 18 genes, showed a 5.26-fold enrichment, and had an FDR of $1.57 \times 10{-}5$. The term encompasses several chemokine receptors that guide immune-cell movement between the blood, lymphoid tissues, and sites of inflammation. These included CCR3, CCR4, CCR6, CCR7, CCR9, CXCR5 and CXCR6. CCR7 regulates the migration of naïve and central-memory T cells and dendritic cells to lymphoid tissues. CXCR5 and GPR183 are associated with migration within lymphoid follicles, while CCR4, CCR6, CCR9, and CXCR6 define distinct T-cell and other lymphocyte subsets with characteristic tissue-homing properties. The term also contained the chemokines XCL1, XCL2, CCL20 and CCL28, together with the migration-related genes SEMA5A, LEF1, KIT, ACKR3, CCN3 and EPHA2. The coordinated decrease in these genes indicates a marked change in the transcriptional programs that regulate lymphocyte positioning and immune-cell trafficking.

Many of the receptors in this term are expressed by T-cell and other lymphocyte populations. Their reduced expression, therefore, fits with the broader decrease in circulating lymphocyte-associated genes observed in the immune-response and T-cell categories. Severe COVID-19 has been associated with substantial loss and redistribution of circulating lymphocyte populations, along with major changes in peripheral immune cell composition (Prebensen et al., 2023; Wilk et al., 2020).

Positive regulation of T-cell activation

Positive regulation of T-cell activation contained 12 genes, showed an 8.45-fold enrichment, and had an FDR of 2.92 × 10−5. Most genes in this term were MHC class II genes, including HLA-DPA1, HLA-DPB1, HLA-DQA1, HLA-DQA2, HLA-DQB2, HLA-DRA, HLA-DRB1, HLA-DMB, and HLA-DOA. The term also included CD28, LCK, and SIRPG. CD28 provides a central co-stimulatory signal required for effective T-cell activation. LCK is a proximal tyrosine kinase that initiates signaling downstream of the T-cell receptor, while SIRPG contributes to interactions between T cells and antigen-presenting cells.

The combined reduction in MHC class II, co-stimulatory, and proximal T-cell-signaling genes links reduced antigen presentation to weaker T-cell activation programs. Saichi et al. (2021) reported disrupted communication between dendritic cells and T cells in severe COVID-19, alongside reduced expression of MHC class II genes in antigen-presenting cells. Prebensen et al. (2023) also observed reduced class II HLA expression and T-cell activation programs, particularly in severe disease.

This term, therefore, connects two major findings in the downregulated gene set: reduced capacity for antigen display by circulating antigen-presenting cells and lower expression of genes required for T-cell activation.

T-cell receptor signaling pathway

The T-cell receptor signaling pathway contained 20 genes, showed a 4.33-fold enrichment, and had an FDR of 4.85 × 10−5. The gene set included core components of the T-cell receptor complex, including CD3D, CD3E, CD3G, and CD247. These molecules transmit signals generated when the T-cell receptor recognizes antigen. The term also included the co-receptor genes CD4, CD8A, CD8B and CD8B2, together with the co-stimulatory receptor CD28. Intracellular signaling genes included LCK, ITK, THEMIS, and SKAP1, which coordinate early receptor signaling, thymocyte development, and downstream activation. Transcriptional and cell-identity genes included GATA3 and ZNF683, while HLA-DPB1 and HLA-DRB1 linked T-cell signaling with antigen presentation. The coordinated reduction of these genes indicates a lower T-cell-associated transcriptional signal in severe COVID-19. In particular, reduced expression of CD3D, CD3E, CD3G, CD247, LCK, ITK and CD28 points to lower representation of the molecular machinery required for antigen recognition and signal propagation in T cells. Previous studies have reported lymphopenia and major changes in circulating T-cell populations during severe COVID-19. Wilk et al. (2020) described extensive reconfiguration of peripheral lymphocyte populations, while longitudinal whole-blood analysis showed reduced T-cell receptor signaling at multiple time points and decreased CD8 T-cell proportions in severe disease (Prebensen et al., 2023). The present results closely reproduce this pattern at the transcriptomic level.

Together, the top ten downregulated gene ontology terms define a whole-blood transcriptional state characterized by reduced expression of ribosomal and translation-related genes, weaker MHC class II antigen-presentation programs, altered immune-cell migration, and lower T-cell-associated expression. The strongest signal involved the ribosome. Cytoplasmic translation, translation, ribosomal small-subunit biogenesis, negative regulation of myoblast fusion, and striated muscle contraction were largely driven by the same coordinated decrease in RPL and RPS genes. This indicates that reduced expression of the protein-synthesis machinery was the dominant feature of the downregulated gene set. A second major pattern involved the adaptive immune response. The reduction in HLA-DP, HLA-DQ, and HLA-DR genes linked the immune response, antigen assembly, and T-cell activation categories. Lower expression of these genes

indicates a broad reduction in class II antigen-presentation programs. The downregulation of CD3D, CD3E, CD3G, CD247, CD4, CD8A, CD8B, CD28, LCK, ITK, and THEMIS further identifies a weaker T-cell receptor and co-stimulatory program. At the same time, reduced expression of CCR3, CCR4, CCR6, CCR7, CCR9, CXCR5, and CXCR6 indicates altered representation and migration programs of circulating lymphocyte populations. Overall, these findings show that severe COVID-19 was associated with a broad reduction in ribosomal, antigen-presentation, lymphocyte-trafficking, and T-cell-signaling transcripts. When considered alongside the strong upregulation of neutrophil and myeloid-inflammatory genes, the results define an imbalanced whole-blood immune response in which enhanced innate immune activation is accompanied by reduced circulating adaptive immune programs. This integrated pattern agrees with previous whole-blood and single-cell studies of severe COVID-19 (Prebensen et al., 2023; Saichi et al., 2021; Wilk et al., 2020).

KEGG pathway analysis reveals neutrophil-driven immunothrombosis and suppression of adaptive immune programs in severe COVID-19

KEGG analysis (Figure 5B) revealed a pronounced shift from adaptive immune and biosynthetic programs towards neutrophil-dominated inflammation and immunothrombosis in the whole blood of patients with severe COVID-19. Among the upregulated genes, neutrophil extracellular trap formation was the most significantly enriched pathway and contained the largest number of differentially expressed genes. Severe COVID-19 is characterized by neutrophilia, expansion of immature neutrophil populations, and emergency myelopoiesis, which together increase the representation of neutrophil-associated transcripts in whole blood (Schulte-Schrepping et al., 2020; Wilk et al., 2020). Excessive formation of neutrophil extracellular traps (NETs), comprising extracellular DNA, histones, and neutrophil granule proteins, can damage pulmonary and vascular tissues while providing a scaffold for platelet adhesion and thrombus formation. Consistent with this interpretation, NET abundance is associated with respiratory failure and pulmonary immunothrombosis in severe COVID-19 (Middleton et al., 2020).

The concurrent enrichment of complement and coagulation cascades, integrin signalling and ECM-receptor interaction further indicates coordinated activation of neutrophils, platelets and vascular adhesion pathways. Complement-derived mediators promote neutrophil recruitment and activation, whereas NET-associated tissue factor and extracellular chromatin stimulate thrombin generation and platelet aggregation. This reciprocal complement-NET-coagulation axis is a major mechanism linking systemic inflammation to the pulmonary microvascular thrombosis and endothelial injury observed in severe COVID-19 (Skendros et al., 2020). Enrichment of integrin and extracellular. matrix pathways may similarly reflect enhanced leukocyte adhesion, platelet-leukocyte aggregation, and inflammatory-cell migration across the activated vascular endothelium.

The enrichment of cell-cycle pathways is consistent with the emergence of proliferating or developmentally immature myeloid cells during emergency hematopoiesis, rather than with the proliferation of mature circulating neutrophils. The accompanying p53 signaling signature suggests activation of cellular stress, DNA damage, and apoptosis-related programs during severe systemic inflammation. Enrichment of systemic lupus erythematosus, alcoholism, viral carcinogenesis, and transcriptional misregulation in cancer should be interpreted as reflecting shared histone, chromatin, and cell-death-associated genes rather than the presence of these conditions. In particular, histone transcripts contribute to several of these KEGG categories and may be associated with increased granulopoiesis and chromatin release during NET formation.

By contrast, the downregulated genes were predominantly associated with the ribosome and coronavirus disease (COVID-19) pathways. The latter KEGG category contains numerous ribosomal protein genes; therefore, the simultaneous enrichment of both terms primarily indicates reduced expression of translational machinery rather than suppression of COVID-19-related biology. This pattern may reflect stress-associated translational reprogramming together with the altered cellular composition of severe COVID-19 blood, particularly the expansion of immature myeloid populations and depletion of lymphocytes. Multi-omic studies have similarly demonstrated extensive metabolic and transcriptional remodeling of circulating immune cells in severe disease (Bernardes et al., 2020).

Downregulation of haematopoietic cell lineage, Th17-cell differentiation, Th1- and Th2-cell differentiation, antigen processing and presentation, and cell-adhesion molecule interaction indicates marked disruption of adaptive immune and antigen-presenting-cell programmes. Severe COVID-19 is associated with lymphopenia, reduced circulating T-cell populations and decreased HLA class II expression in monocytes and dendritic cells (Arunachalam et al., 2020; Wilk et al., 2020). Reduced antigen-processing and presentation may weaken effective T-cell priming, whereas lower Th1, Th2 and Th17 differentiation signatures probably reflect both numerical loss and functional reprogramming of circulating $CD4^+$ T cells. The downregulation of the intestinal immune network for IgA production and related immune-disease pathways, including asthma and inflammatory bowel disease, further suggests depletion or redistribution of B-cell, T-cell, and antigen-presenting-cell programs shared with mucosal immunity. Single-cell multi-omic analysis has likewise identified extensive alterations in B-cell, plasmablast, and immunoglobulin-associated responses during symptomatic and severe COVID-19 (Stephenson et al., 2021).

Collectively, these results define severe COVID-19 as a state of innate immune excess coupled with adaptive immune suppression. Upregulation of NET formation, complement, coagulation, integrin, and extracellular matrix pathways supports a neutrophil-centered immunothrombotic response, whereas suppression of ribosomal, antigen presentation, lymphocyte differentiation, and IgA-associated pathways indicate impaired biosynthetic and adaptive immune functions. This coordinated transcriptional reprogramming provides a mechanistic link between systemic inflammation, vascular thrombosis, lymphopenia, and defective antiviral immune regulation in severe COVID-19.

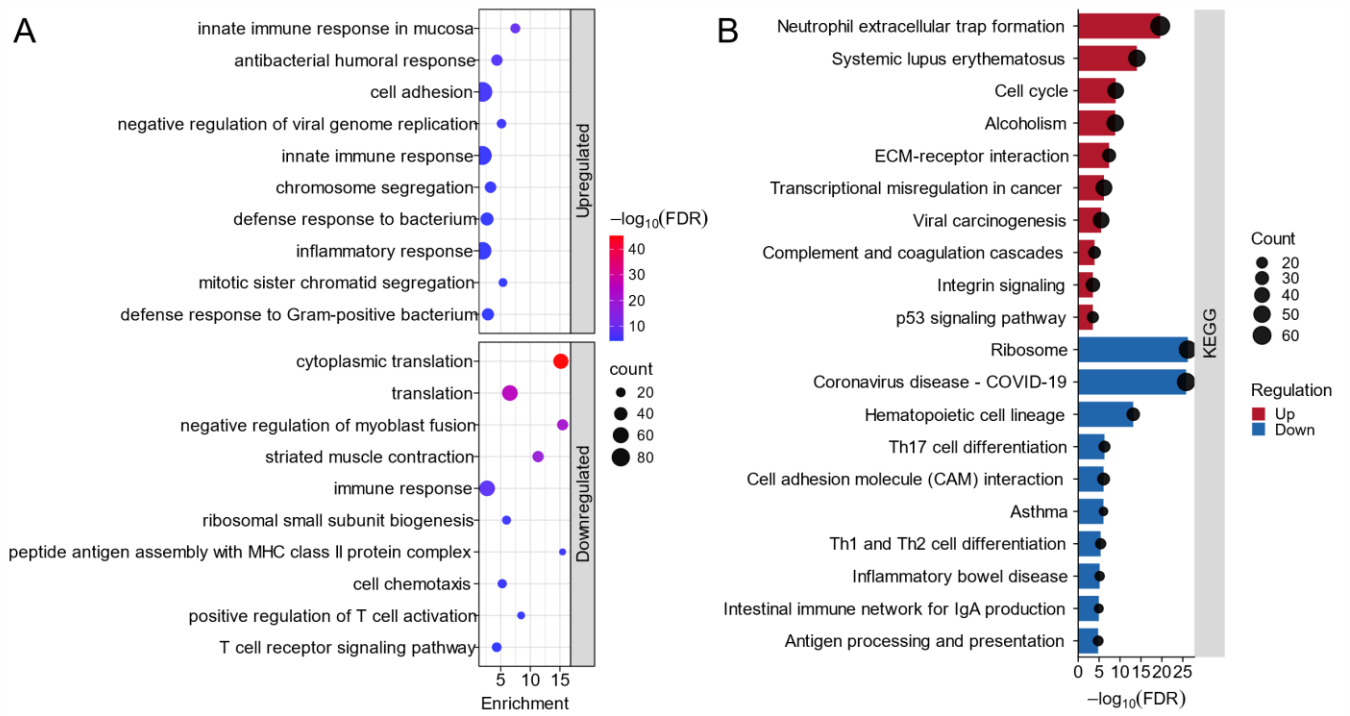

Figure 5. Functional enrichment of genes differentially expressed in severe COVID-19. (A) Gene Ontology biological-process enrichment analysis of genes upregulated (upper panel) and downregulated (lower panel) in severe COVID-19 relative to healthy donors. The ten leading terms are shown for each gene set. The horizontal axis represents fold enrichment, circle size indicates the number of genes assigned to each term, and color denotes significance as −log10(false discovery rate (FDR)). (B) Kyoto Encyclopedia of Genes and Genomes pathway enrichment analysis of upregulated and downregulated genes. Red and blue bars represent pathways enriched among upregulated and downregulated genes, respectively. Bar length indicates −log10(FDR), and black-circle size represents the number of genes assigned to each pathway.

Protein-interaction network identifies highly connected candidate hub genes

The differentially expressed protein-coding genes formed a highly connected protein-protein association network in STRING (Figure 6A). Degree-based analysis using cytoHubba identified CD4, FN1, CD8A, UBA52, RPS27A, CDK1, CXCL8, IL10, MMP9, and JUN as the ten most highly connected genes in the network (Figure 6B). Node color represents Degree centrality, ranging from yellow to dark red, with darker red indicating a greater number of direct network connections. CD4 and FN1 showed the darkest red color and therefore had the highest degree values, while CD8A, UBA52, and RPS27A also showed relatively high connectivity. CDK1, CXCL8, and IL10 had intermediate degree values, whereas MMP9 and JUN had comparatively lower degree values within the top ten network. Despite these differences, all ten genes occupied highly connected positions relative to the remaining differentially expressed genes.

The biological functions of these hub genes were consistent with the major transcriptional patterns identified in the enrichment analysis. CXCL8, MMP9, JUN, and IL10 represented inflammatory, chemotactic, tissue remodeling, stress response, and immune regulatory processes. CXCL8 is an important chemokine involved in neutrophil recruitment, while MMP9

contributes to extracellular-matrix degradation and inflammatory tissue remodeling. JUN is a component of the AP-1 transcriptional complex and participates in cellular stress and inflammatory signaling, whereas IL10 is associated with the regulation of excessive immune responses. Their presence among the hub genes supports the strong inflammatory and neutrophil-associated transcriptional signature observed in severe COVID-19. However, their network connectivity reflects functional association and does not directly demonstrate increased protein abundance or activity.

The high connectivity of FN1 and MMP9 further supports the enrichment of cell-adhesion and extracellular-matrix-associated pathways. FN1 encodes fibronectin, a major extracellular-matrix protein involved in cell attachment and matrix organization, whereas MMP9 contributes to matrix breakdown and remodeling. These genes may therefore connect inflammatory responses with the vascular and extracellular-matrix-associated changes identified in the whole-blood transcriptome. CDK1, a central regulator of cell-cycle progression, was also identified as a hub, consistent with the enrichment of chromosome-segregation, mitotic, and cell-cycle-related programs. This proliferative signature may reflect an increased representation of cycling immune or hematopoietic precursor cells in severe disease rather than the proliferation of mature circulating neutrophils.

In contrast, CD4 and CD8A link the network to the reduced adaptive immune and T-cell-associated transcriptional programs observed in the downregulated gene set. Their high network degree should not be interpreted as evidence of increased T-cell activity. Instead, it indicates that highly connected components of the adaptive immune network were underrepresented in the whole blood of patients with severe COVID-19. Similarly, UBA52 and RPS27A, which encode ubiquitin-ribosomal fusion proteins, connect the network to the prominent reduction in ribosomal and translation-related transcripts. Their central positions may reflect the broad involvement of ribosomal proteins in protein synthesis and cellular protein homeostasis.

Overall, the hub-gene network integrates the main biological patterns identified in this study: inflammatory and neutrophil-associated responses, extracellular matrix remodeling, cell cycle activity, reduced T-cell-associated expression, and altered ribosomal programs.

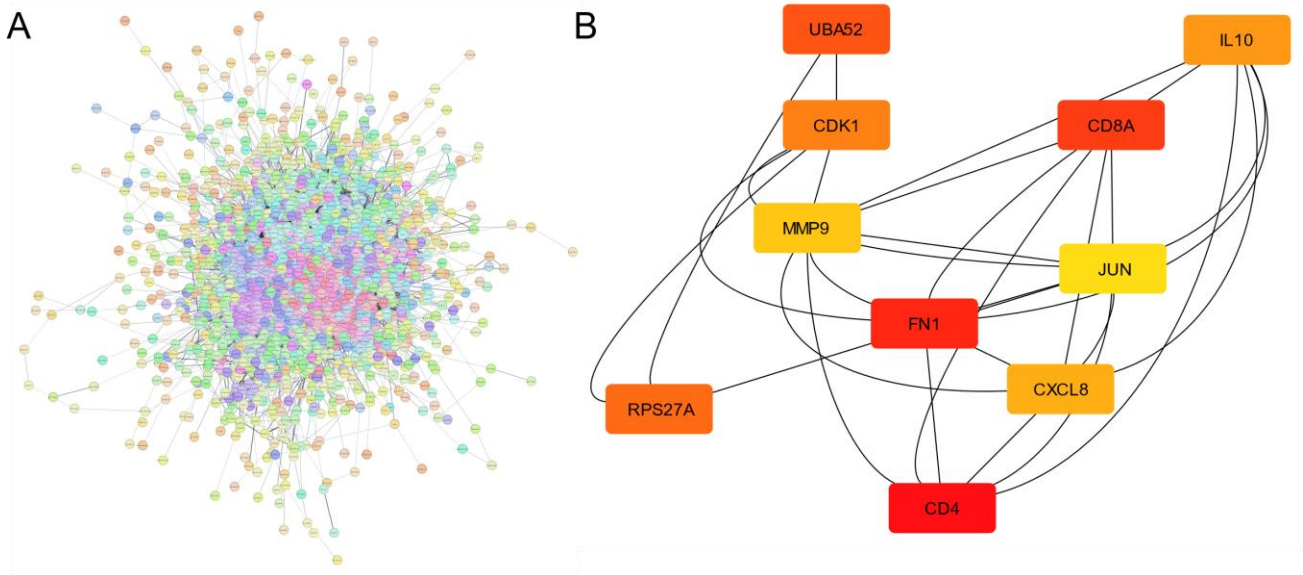

Figure 6. Protein-protein association network and identification of candidate hub genes. (A) Protein-protein association network constructed from significantly differentially expressed protein-coding genes

using STRING with a minimum combined confidence score of 0.700. Nodes represent proteins, and edges represent high-confidence known or predicted functional associations. (B) The ten candidate hub genes identified using the Degree algorithm in cytoHubba were CD4, FN1, CD8A, UBA52, RPS27A, CDK1, CXCL8, IL10, MMP9, and JUN. Node color represents Degree centrality, ranging from yellow to dark red, with darker red indicating more direct network connections.

Limitations of study

This study has several limitations. First, the analysis was based on a single publicly available dataset, which may limit the generalizability of the findings across different populations, clinical settings, and SARS-CoV-2 variants. Although all available samples were included, the healthy-control group contained only 10 individuals. This smaller control group may limit the estimation of normal biological variation and reduce confidence in detecting modest gene-expression differences. The absence of patients with asymptomatic, mild, or moderate disease also prevented us from determining whether the identified transcriptional changes developed progressively with disease severity. Because bulk whole-blood RNA sequencing measures the combined expression of multiple circulating cell populations, the observed changes may reflect both altered gene regulation and differences in blood cell composition. Potential confounding factors, including age, sex, comorbidities, disease duration, treatment exposure, and technical variation, were not included in the differential-expression model. In addition, the study was entirely computational and was not validated in an independent RNA-seq cohort or experimentally confirmed by qRT-PCR, proteomics, flow cytometry, single-cell sequencing, or functional assays. Therefore, the differentially expressed genes and hub genes should be interpreted as exploratory candidate transcriptional markers rather than validated biomarkers or causal regulators of severe COVID-19. Similarly, degree centrality identifies highly connected genes within a protein-association network but does not establish disease specificity, clinical predictive value, biological causality, or therapeutic relevance. The enrichment and network analyses therefore identify biological associations rather than direct mechanisms, and further validation in independent clinical cohorts and experimental systems is required before these genes can be considered reliable biomarkers or therapeutic targets.

Conclusion

This study provides an integrated view of the severe COVID-19 whole-blood transcriptome. Rather than showing isolated pathway changes, the results indicate a coordinated imbalance between activated innate immune programs and reduced adaptive immune and biosynthetic programs. Upregulated genes point to neutrophil-associated antimicrobial defense, inflammation, antiviral activity, platelet-vascular interaction, extracellular matrix remodeling, and cell cycle-related activity. In contrast, downregulated genes point to reduced ribosomal and translational activity, weaker MHC class II antigen presentation, altered lymphocyte trafficking, and reduced T-cell receptor signaling. Together, these patterns suggest that severe COVID-19 blood is shaped by both inflammatory activation and the loss or reprogramming of key immune cell populations. Because the study used bulk whole blood, the findings should be interpreted as a combined signal of transcriptional regulation and changes in circulating blood-cell composition. This synthesis links the major molecular features of severe COVID-19, innate inflammation, immunothrombosis, lymphocyte dysfunction, and reduced protein-synthesis programs within one transcriptomic framework.

Future studies should validate these transcriptomic findings in larger, clinically well-annotated cohorts, including data on age, sex, comorbidities, treatments, disease stage, and clinical outcomes. Single-cell and spatial transcriptomic approaches would help separate true gene-regulatory changes from shifts in blood-cell composition and identify the specific immune-cell populations driving the neutrophil, platelet-vascular, T-cell, antigen-presentation, and ribosomal signatures observed here. Longitudinal sampling will also be important to determine whether these pathways change during recovery or progression, and whether selected genes or pathway modules can serve as biomarkers of severity, prognosis, or therapeutic response in severe COVID-19.

References:

Ackermann, M., Verleden, S. E., Kuehnel, M., Haverich, A., Welte, T., Laenger, F., Vanstapel, A., Werlein, C., Stark, H., Tzankov, A., Li, W. W., Li, V. W., Mentzer, S. J., & Jonigk, D. (2020). Pulmonary Vascular Endothelialitis, Thrombosis, and Angiogenesis in Covid-19. The New England journal of medicine, 383(2), 120–128. https://doi.org/10.1056/NEJMoa2015432

Anders, S., & Huber, W. (2010). Differential expression analysis for sequence count data. Genome Biology, 11(10), R106. https://doi.org/10.1186/gb-2010-11-10-r106

Andrews, S. (2010). FastQC: A quality control tool for high throughput sequence data. Babraham Bioinformatics. https://www.bioinformatics.babraham.ac.uk/projects/fastqc/

Arunachalam, P. S., Wimmers, F., Mok, C. K. P., Perera, R. A. P. M., Scott, M., Hagan, T., Sigal, N., Feng, Y., Bristow, L., Tak-Yin Tsang, O., Wagh, D., Coller, J., Pellegrini, K. L., Kazmin, D., Alaaeddine, G., Leung, W. S., Chan, J. M. C., Chik, T. S. H., Choi, C. Y. C., Huerta, C., … Pulendran, B. (2020). Systems biological assessment of immunity to mild versus severe COVID-19 infection in humans. *Science (New York, N.Y.)*, *369*(6508), 1210–1220. https://doi.org/10.1126/science.abc6261

Aschenbrenner, A. C., Mouktaroudi, M., Kraemer, B., Oestreich, M., Antonakos, N., Nuesch-Germano, M., ... & Ulas, T. (2021). Disease severity-specific neutrophil signatures in blood transcriptomes stratify COVID-19 patients. *Genome medicine*, *13*(1), 7. https://doi.org/10.1186/s13073-020-00823-5

Bernardes, J. P., Mishra, N., Tran, F., Bahmer, T., Best, L., Blase, J. I., Bordoni, D., Franzenburg, J., Geisen, U., Josephs-Spaulding, J., Köhler, P., Künstner, A., Rosati, E., Aschenbrenner, A. C., Bacher, P., Baran, N., Boysen, T., Brandt, B., Bruse, N., Dörr, J., … Deutsche COVID-19 Omics Initiative (DeCOI) (2020). Longitudinal Multi-omics Analyses Identify Responses of Megakaryocytes, Erythroid Cells, and Plasmablasts as Hallmarks of Severe COVID-19. *Immunity*, *53*(6), 1296–1314.e9. https://doi.org/10.1016/j.immuni.2020.11.017

Conesa, A., Madrigal, P., Tarazona, S., Gomez-Cabrero, D., Cervera, A., McPherson, A., Szcześniak, M. W., Gaffney, D. J., Elo, L. L., Zhang, X., & Mortazavi, A. (2016). A survey of best practices for RNA-seq data analysis. Genome biology, 17, 13. https://doi.org/10.1186/s13059-016-0881-8

Dennis Jr, G., Sherman, B. T., Hosack, D. A., Yang, J., Gao, W., Lane, H. C., & Lempicki, R. A. (2003). DAVID: database for annotation, visualization, and integrated discovery. Genome biology, 4(9), R60. https://doi.org/10.1186/gb-2003-4-9-r60

Figueiredo, V. C., & McCarthy, J. J. (2019). Regulation of Ribosome Biogenesis in Skeletal Muscle Hypertrophy. *Physiology (Bethesda, Md.)*, *34*(1), 30–42. https://doi.org/10.1152/physiol.00034.2018

Goecks, J., Nekrutenko, A., Taylor, J., & The Galaxy Team. (2010). Galaxy: A comprehensive approach for supporting accessible, reproducible, and transparent computational research in the life sciences. Genome Biology, 11(8), R86. https://doi.org/10.1186/gb-2010-11-8-r86

Homma, S. T., Wang, X., Frere, J. J., Gower, A. C., Zhou, J., Lim, J. K., tenOever, B. R., & Zhou, L. (2024). Respiratory SARS-CoV-2 Infection Causes Skeletal Muscle Atrophy and Long-Lasting Energy Metabolism Suppression. *Biomedicines*, *12*(7), 1443. https://doi.org/10.3390/biomedicines12071443

Li, H., Handsaker, B., Wysoker, A., Fennell, T., Ruan, J., Homer, N., Marth, G., Abecasis, G., Durbin, R., & 1000 Genomes Project Data Processing Subgroup. (2009). The Sequence Alignment/Map format and SAMtools. Bioinformatics, 25(16), 2078-2079. https://doi.org/10.1093/bioinformatics/btp352

Liao, Y., Smyth, G. K., & Shi, W. (2014). featureCounts: An efficient general purpose program for assigning sequence reads to genomic features. Bioinformatics, 30(7), 923-930. https://doi.org/10.1093/bioinformatics/btt656

Love, M. I., Huber, W., & Anders, S. (2014). Moderated estimation of fold-change and dispersion for RNA-seq data with DESeq2. Genome Biology, 15(12), 550. https://doi.org/10.1186/s13059-014-0550-8

Lucas, C., Wong, P., Klein, J., Castro, T. B. R., Silva, J., Sundaram, M., Ellingson, M. K., Mao, T., Oh, J. E., Israelow, B., Takahashi, T., Tokuyama, M., Lu, P., Venkataraman, A., Park, A., Mohanty, S., Wang, H., Wyllie, A. L., Vogels, C. B. F., Earnest, R., … Iwasaki, A. (2020). Longitudinal analyses reveal immunological misfiring in severe COVID-19. Nature, 584(7821), 463–469. https://doi.org/10.1038/s41586-020-2588-y

Lyu, P., & Jiang, H. (2022). RNA-Sequencing Reveals Upregulation and a Beneficial Role of Autophagy in Myoblast Differentiation and Fusion. *Cells*, *11*(22), 3549. https://doi.org/10.3390/cells11223549

Meacci, E., Pierucci, F., & Garcia-Gil, M. (2022). Skeletal Muscle and COVID-19: The Potential Involvement of Bioactive Sphingolipids. *Biomedicines*, *10*(5), 1068. https://doi.org/10.3390/biomedicines10051068

Middleton, E. A., He, X. Y., Denorme, F., Campbell, R. A., Ng, D., Salvatore, S. P., Mostyka, M., Baxter-Stoltzfus, A., Borczuk, A. C., Loda, M., Cody, M. J., Manne, B. K., Portier, I., Harris, E. S., Petrey, A. C., Beswick, E. J., Caulin, A. F., Iovino, A., Abegglen, L. M., Weyrich, A. S., … Yost, C. C. (2020). Neutrophil extracellular traps contribute to immunothrombosis in COVID-19 acute respiratory distress syndrome. Blood, 136(10), 1169–1179. https://doi.org/10.1182/blood.2020007008

Prebensen, C., Lefol, Y., Myhre, P. L., Lüders, T., Jonassen, C., Blomfeldt, A., ... & Berdal, J. E. (2023). Longitudinal whole blood transcriptomic analysis characterizes neutrophil activation and interferon signaling in moderate and severe COVID-19. *Scientific reports*, *13*(1), 10368. https://doi.org/10.1038/s41598-023-37606-y

Qin, C., Zhou, L., Hu, Z., Zhang, S., Yang, S., Tao, Y., Xie, C., Ma, K., Shang, K., Wang, W., & Tian, D. S. (2020). Dysregulation of Immune Response in Patients With Coronavirus 2019 (COVID-19) in Wuhan, China. Clinical infectious diseases : an official publication of the Infectious Diseases Society of America, 71(15), 762–768. https://doi.org/10.1093/cid/ciaa248

Saichi, M., Ladjemi, M. Z., Korniotis, S., Rousseau, C., Ait Hamou, Z., Massenet-Regad, L., Amblard, E., Noël, F., Marie, Y., Bouteiller, D., Medvedovic, J., Pène, F., & Soumelis, V. (2021). Single-cell RNA sequencing of blood antigen-presenting cells in severe COVID-19

reveals multi-process defects in antiviral immunity. Nature Cell Biology, 23(5), 538–551. https://doi.org/10.1038/s41556-021-00681-2

Schulte-Schrepping, J., Reusch, N., Paclik, D., Baßler, K., Schlickeiser, S., Zhang, B., Krämer, B., Krammer, T., Brumhard, S., Bonaguro, L., De Domenico, E., Wendisch, D., Grasshoff, M., Kapellos, T. S., Beckstette, M., Pecht, T., Saglam, A., Dietrich, O., Mei, H. E., Schulz, A. R., … Deutsche COVID-19 OMICS Initiative (DeCOI) (2020). Severe COVID-19 Is Marked by a Dysregulated Myeloid Cell Compartment. *Cell*, *182*(6), 1419–1440.e23. https://doi.org/10.1016/j.cell.2020.08.001

Shiraishi, C., Matsumoto, A., Ichihara, K., Yamamoto, T., Yokoyama, T., Mizoo, T., Hatano, A., Matsumoto, M., Tanaka, Y., Matsuura-Suzuki, E., Iwasaki, S., Matsushima, S., Tsutsui, H., & Nakayama, K. I. (2023). RPL3L-containing ribosomes determine translation elongation dynamics required for cardiac function. *Nature communications*, *14*(1), 2131. https://doi.org/10.1038/s41467-023-37838-6

Skendros, P., Mitsios, A., Chrysanthopoulou, A., Mastellos, D. C., Metallidis, S., Rafailidis, P., Ntinopoulou, M., Sertaridou, E., Tsironidou, V., Tsigalou, C., Tektonidou, M., Konstantinidis, T., Papagoras, C., Mitroulis, I., Germanidis, G., Lambris, J. D., & Ritis, K. (2020). Complement and tissue factor-enriched neutrophil extracellular traps are key drivers in COVID-19 immunothrombosis. *The Journal of clinical investigation*, *130*(11), 6151–6157. https://doi.org/10.1172/JCI141374

Stephenson, E., Reynolds, G., Botting, R. A., Calero-Nieto, F. J., Morgan, M. D., Tuong, Z. K., Bach, K., Sungnak, W., Worlock, K. B., Yoshida, M., Kumasaka, N., Kania, K., Engelbert, J., Olabi, B., Spegarova, J. S., Wilson, N. K., Mende, N., Jardine, L., Gardner, L. C. S., Goh, I., … Haniffa, M. (2021). Single-cell multi-omics analysis of the immune response in COVID-19. *Nature medicine*, *27*(5), 904–916. https://doi.org/10.1038/s41591-021-01329-2

Wang, L., Wang, S., & Li, W. (2012). RSeQC: Quality control of RNA-seq experiments. Bioinformatics, 28(16), 2184-2185. https://doi.org/10.1093/bioinformatics/bts356

Wen, Y., Alimov, A. P., & McCarthy, J. J. (2016). Ribosome Biogenesis is Necessary for Skeletal Muscle Hypertrophy. *Exercise and sport sciences reviews*, *44*(3), 110–115. https://doi.org/10.1249/JES.0000000000000082

Wilk, A. J., Rustagi, A., Zhao, N. Q., Roque, J., Martínez-Colón, G. J., McKechnie, J. L., Ivison, G. T., Ranganath, T., Vergara, R., Hollis, T., Simpson, L. J., Grant, P., Subramanian, A., Rogers, A. J., & Blish, C. A. (2020). A single-cell atlas of the peripheral immune response in patients with severe COVID-19. Nature Medicine, 26(7), 1070–1076. https://doi.org/10.1038/s41591-020-0944-y

World Health Organization. (2025, November 27). Coronavirus disease (COVID-19). https://www.who.int/news-room/fact-sheets/detail/coronavirus-disease-%28covid-19%29